Inorg. Chem. **2003**, *42*, 8262–8269

The Pacman Effect: A Supramolecular Strategy for Controlling the Excited-State Dynamics of Pillared Cofacial Bisporphyrins

Christopher J. Chang, Zhi-Heng Loh, Yongqi Deng, and Daniel G. Nocera*

Department of Chemistry, 6-335, Massachusetts Institute of Technology, 77 Massachusetts Avenue, Cambridge, Massachusetts 02139-4307

Received July 1, 2003

The molecular recognition properties of dizinc(II) bisporphyrin anchored by dibenzofuran (DPD), Zn_2(DPD) (**1**), were evaluated as a strategy for utilizing the Pacman effect to control the excited-state properties of cofacial bisporphyrin motifs. Crystallographic studies establish that DPD furnishes a cofacial system with vertical flexibility and horizontal preorganization. The structure determination of a substrate-bound DPD species, Zn_2(DPD)(2-aminopyrimidine) (**2**), completes a set of structurally homologous zinc(II) porphyrin host and host–guest complexes, which offer a direct structural comparison for the Pacman effect upon substrate complexation. Binding studies reveal that pyrimidine encapsulation by the DPD framework is accompanied by a markedly reduced entropic penalty ($\sim$60 J $mol^{-1}K^{-1}$) with respect to traditional face-to-face bisporphyrin systems, giving rise to a smaller conformational energy cost upon substrate binding. Transient absorption spectroscopy reveals that substrate encapsulation within the DPD cleft dramatically affects excited-state dynamics of cofacial bisporphyrins. The emission lifetime of host–guest complex **2** increases by more than an order of magnitude compared to free host **1**. In the absence of the guest, the excited-state dynamics are governed by torsional motion of the porphyrin rings about the aryl ring of the DPD pillar. Host–guest binding attenuates this conformational flexibility, thereby removing efficient nonradiative decay pathways. Taken together, these findings support the exceptional ability of the DPD system to structurally accommodate reaction intermediates during catalytic turnover and provide a novel supramolecular approach toward developing a reaction chemistry derived directly from the excited states of Pacman constructs.

Introduction

The unrivaled capacity of enzymes to perform sophisticated chemical transformations derives largely from their substantial structural flexibility.[1−3] By modulating their physical shape, enzymatic systems are able to exquisitely direct substrate binding, activation, and/or product release.[1,2] The elaborate host−guest chemistry exhibited by complex biological systems provides motivation for the creation of simple synthetic constructs to catalyze new chemical transformations of substrates docked at an active site.[4−7] One such construct consists of two porphyrins linked in a face-to-face arrangement by a rigid anthracene or biphenylene pillar, so-called "Pacman" porphyrins, that form molecular clefts for the binding and activation of a variety of small molecules (e.g., O_2, N_2, and H_2).[7−22]

We have explored the structural limits of flexibility within the Pacman motif in order to expand the use of these and

* Author to whom correspondence should be addressed. E-mail: nocera@mit.edu.

(1) Jencks, W. P. *Catalysis in Chemistry and Enzymology*; Dover: Mineola, NY, 1987.
(2) Fersht, A. *Enzyme Structure and Mechanism*, 2nd ed.; W. H. Freeman: New York, 1985.
(3) Lippard, S. J.; Berg, J. M. *Principles of Bioinorganic Chemistry*; University Science Books: Mill Valley, CA, 1994.
(4) Sanders, J. K. M. *Chem.—Eur. J.* **1998**, *4*, 1378−1383.
(5) Kirby, A. J. *Angew. Chem., Int. Ed. Engl.* **1996**, *35*, 707−724.
(6) Breslow, R. *Chemtracts* **2002**, *15*, 59−68.
(7) Collman, J. P.; Wagenknecht, P. S.; Hutchison, J. E. *Angew. Chem., Int. Ed. Engl.* **1994**, *33*, 1537−1554.
(8) Chang, C. K.; Abdalmuhdi, I. *J. Org. Chem.* **1983**, *48*, 5388−5390.
(9) Chang, C. K.; Liu, H. Y.; Abdalmuhdi, I. *J. Am. Chem. Soc.* **1984**, *106*, 2725−2726.
(10) Chang, C. K.; Abdalmuhdi, I. *Angew. Chem., Int. Ed. Engl.* **1984**, *23*, 164−165.
(11) Lui, H.-Y.; Abdalmuhdi, I.; Chang, C. K.; Anson, F. C. *J. Phys. Chem.* **1985**, *89*, 665−670.
(12) Ni, C.-L.; Abdalmuhdi, I.; Chang, C. K.; Anson, F. C. *J. Phys. Chem.* **1987**, *91*, 1158−1166.
(13) Collman, J. P.; Hutchison, J. E.; Lopez, M. A.; Tabard, A.; Guilard, R.; Seok, W. K.; Ibers, J. A.; L'Her, M. *J. Am. Chem. Soc.* **1992**, *114*, 9869−9877.
(14) Collman, J. P.; Hutchison, J. E.; Lopez, M. A.; Guilard, R. *J. Am. Chem. Soc.* **1992**, *114*, 8066−8073.
(15) Collman, J. P.; Hutchison, J. E.; Ennis, M. S.; Lopez, M. A.; Guilard, R. *J. Am. Chem. Soc.* **1992**, *114*, 8074−8080.

10.1021/ic034750w CCC: $25.00
Published on Web 11/11/2003

related platforms for catalytic multielectron reactivity, especially as it pertains to our interest in proton-coupled electron transfer (PCET)[23−33] and attendant PCET-mediated activation of oxygen and related small-molecule substrates.[34−38] To this end, we have recently developed methods for the assembly of new cofacial bisporphyrins affixed to xanthene and dibenzofuran pillars. The DPX (diporphyrin xanthene)[39−42] and DPD (diporphyrin dibenzofuran)[40−43] architectures afford a wide range of vertical pocket sizes and flexibilities while maintaining a face-to-face arrangement of macrocyclic subunits. In particular, the DPD system provided direct support for the Pacman effect in a single framework.[43] A comparative structural analysis of dizinc(II) and diiron(III) μ-oxo complexes of DPD demonstrated the exceptional ability of this platform to open and close its binding pocket by a vertical distance of more than 4 Å.[43] Efficient oxygen-activation chemistry is observed when such cofacial structural motifs minimize lateral displacement over this large range of vertical motion. Dicobalt(II) complexes of both DPX and DPD are effective electrocatalysts for the four-electron reduction of oxygen to water despite their roughly 4 Å difference in metal−metal distances,[44] and the diiron(III) μ-oxo complex of DPD shows superior reactivity compared to rigid or unbridged counterparts for the photooxidation of organic substrates under mild conditions.[40,45] This latter result suggests not only that the vertical Pacman flexibility of the molecules mimics the induced fit that is so crucial to enzyme catalysis but also that the Pacman effect has consequences for photoinduced reaction chemistry as well.

Our aim of developing a photochemistry for the Pacman motif is predicated on an intimate understanding of fundamental excited-state properties. To date, photocatalytic cycles involving cofacial bisporphyrins employ the Pacman construct as a precatalyst;[40,45] in this case, the absorption of a photon unmasks an active ground-state catalyst for substrate conversion. In contrast, the direct use of the Pacman excited state to promote multielectron photochemistry has been elusive owing to the need for a long-lived excited state to participate in the reaction with the substrate. This challenge is highlighted by our recent studies of the excited-state dynamics of dipalladium(II) Pacman porphyrins.[46] Specifically, the wedge-shaped structure of Pd_2(DPD) allows for torsional librations about the C_{meso}—$C_{aryl\ bridge}$ bond, which lead to an enhancement in the nonradiative decay rate and accordant shortening of the triplet excited-state lifetime compared to the more rigid DPX analogue (18.2(2) μs for Pd_2(DPD), 102(3) μs for Pd_2(DPX)). These results uncover a paradox to the development of Pacman photochemistry; although the large vertical flexibility afforded by the DPD scaffold enhances photocatalytic turnover, the large torsional flexibility associated with this splayed motif has a detrimental effect on its excited-state properties.

The pursuit of direct multielectron photochemistry from Pacman constructs provides an imperative for the discovery of new approaches for tailoring the photophysics of the Pacman excited state. Toward this end, we reasoned that the torsional librations of the DPD Pacman scaffold could be minimized upon binding substrate inside the Pacman cavity. Accordingly, we sought to develop a host−guest chemistry of the DPD platform by using stable adducts that are amenable to structural and spectroscopic scrutiny. Sanders' approach of using multifunctional zinc(II) porphyrin hosts with neutral nitrogen donors to form Lewis acid−base inclusion complexes provided an attractive starting point.[47−63] For our purposes, pyrimidine-based guests were selected for

(16) Collman, J. P.; Ha, Y.; Wagenknecht, P. S.; Lopez, M. A.; Guilard, R. *J. Am. Chem. Soc.* **1993**, *115*, 9080−9088.
(17) Guilard, R.; Lopez, M. A.; Tabard, A.; Richard, P.; Lecomte, C.; Brandès, S.; Hutchison, J. E.; Collman, J. P. *J. Am. Chem. Soc.* **1992**, *114*, 9877−9889.
(18) Guilard, R.; Brandès, S.; Tardieux, C.; Tabard, A.; L'Her, M.; Miry, C.; Gouerec, P.; Knop, Y.; Collman, J. P. *J. Am. Chem. Soc.* **1995**, *117*, 11721−11729.
(19) Le Mest, Y.; L'Her, M.; Hendricks, N. H.; Kim, K.; Collman, J. P. *Inorg. Chem.* **1992**, *31*, 835−847.
(20) Le Mest, Y.; L'Her, M.; Saillard, J. Y. *Inorg. Chim. Acta* **1996**, *248*, 181−191.
(21) Le Mest, Y.; Inisan, C.; Laouenan, A.; L'Her, M.; Talarmain, J.; El Khalifa, M.; Saillard, J. Y. *J. Am. Chem. Soc.* **1997**, *119*, 6905−6106.
(22) Bolze, F.; Gros, C. P.; Drouin, M.; Espinosa, E.; Harvey, P. D.; Guilard, R. *J. Organomet. Chem.* **2002**, *643*−*644*, 89−97.
(23) Chang, C. J.; Chang, M. C. Y.; Damrauer, N. H.; Nocera, D. G. *Biochim. Biophys. Acta*, in press.
(24) Chang, C. J.; Brown, J. D. K.; Chang, M. C. Y.; Baker, E. A.; Nocera, D. G. In *Electron Transfer in Chemistry*; Balzani, V., Ed.; Wiley-VCH: Weinheim, Germany, 2001; Vol. 3.2.4, pp 409−461.
(25) Cukier, R. I.; Nocera, D. G. *Annu. Rev. Phys. Chem.* **1998**, *49*, 337−369.
(26) Yeh, C.-Y.; Miller, S. E.; Carpenter, S. D.; Nocera, D. G. *Inorg. Chem.* **2001**, *40*, 3643−3646.
(27) Deng, Y.; Roberts, J. A.; Peng, S.-M.; Chang, C. K.; Nocera, D. G. *Angew. Chem., Int. Ed. Engl.* **1997**, *36*, 2124−2127.
(28) Kirby, J. P.; Roberts, J. A.; Nocera, D. G. *J. Am. Chem. Soc.* **1997**, *119*, 9230−9236.
(29) Roberts, J. A.; Kirby, J. P.; Wall, S. T.; Nocera, D. G. *Inorg. Chim. Acta* **1997**, *263*, 395−405.
(30) Kirby, J. P.; van Dantzig, N. A.; Chang, C. K.; Nocera, D. G. *Tetrahedron Lett.* **1995**, *36*, 3477−3480.
(31) Roberts, J. A.; Kirby, J. P.; Nocera, D. G. *J. Am. Chem. Soc.* **1995**, *117*, 8051−8052.
(32) Turró, C.; Chang, C. K.; Leroi, G. E.; Cukier, R. I.; Nocera, D. G. *J. Am. Chem. Soc.* **1992**, *114*, 4013−4015.
(33) Damrauer, N. H.; Hodgkiss, J. M.; Rosenthal, J.; Nocera, D. G. *J. Am. Chem. Soc.*, submitted for publication, 2003.
(34) Chang, C. J.; Chng, L. L.; Nocera, D. G. *J. Am. Chem. Soc.* **2003**, *125*, 1866−1876.
(35) Chng, L. L.; Chang, C. J.; Nocera, D. G. *Org. Lett.* **2003**, *5*, 2121−2124.
(36) Chang, C. J.; Yeh, C.-Y.; Nocera, D. G. *J. Org. Chem.* **2002**, *67*, 1403−1406.
(37) Yeh, C.-Y.; Chang, C. J.; Nocera, D. G. *J. Am. Chem. Soc.* **2001**, *123*, 1513−1514.
(38) Chang, C. J.; Loh, Z.-H.; Rosenthal, J.; Shi, C.; Anson, F. C.; Nocera, D. G. Unpublished results.
(39) Chang, C. J.; Deng, Y.; Heyduk, A. F.; Chang, C. K.; Nocera, D. G. *Inorg. Chem.* **2000**, *39*, 959−966.
(40) Chang, C. J.; Baker, E. A.; Pistorio, B. J.; Deng, Y.; Loh, Z.-H.; Miller, S. E.; Carpenter, S. D.; Nocera, D. G. *Inorg. Chem.* **2002**, *41*, 3102−3109.
(41) Chang, C. J.; Deng, Y.; Lee, G.-H.; Peng, S.-M.; Yeh, C.-Y.; Nocera, D. G. *Inorg. Chem.* **2002**, *41*, 3008−3016.
(42) Chng, L. L.; Chang, C. J.; Nocera, D. G. *J. Org. Chem.* **2003**, *68*, 4075−4078.
(43) Deng, Y.; Chang, C. J.; Nocera, D. G. *J. Am. Chem. Soc.* **2000**, *122*, 410−411.
(44) Chang, C. J.; Deng, Y.; Shi, C.; Chang, C. K.; Anson, F. C.; Nocera, D. G. *Chem. Commun.* **2000**, 1355−1356.
(45) Pistorio, B. J.; Chang, C. J.; Nocera, D. G. *J. Am. Chem. Soc.* **2002**, *124*, 7884−7885.
(46) Loh, Z.-H.; Miller, S. E.; Chang, C. J.; Carpenter, S. D.; Nocera, D. G. *J. Phys. Chem. A* **2002**, *106*, 11700−11708.
(47) Sanders, J. K. M. *Pure Appl. Chem.* **2000**, *72*, 2265−2274.
(48) Nakash, M.; Sanders, J. K. M. *J. Chem. Soc., Perkin Trans. 2* **2001**, 2189−2194.
(49) Nakash, M.; Sanders, J. K. M. *J. Org. Chem.* **2000**, *65*, 7266−7271.

investigation. Although few metal-based receptors are known to encapsulate pyrimidine and its derivatives,[64,65] these heterocycles provide an excellent geometric match for the wedge-shaped DPD framework. In this report, we present a detailed structural and spectroscopic investigation of Zn_2DPD−pyrimidine host−guest complexes. Our findings demonstrate that the DPD system provides a Pacman pocket with vertical flexibility and horizontal preorganization that effectively binds substrates with a markedly reduced entropic penalty. Moreover, supramolecular complexation within the cofacial cleft can increase excited-state lifetimes by more than an order of magnitude, revealing that the Pacman effect also affords a facile and effective supramolecular strategy for tuning the excited-state dynamics of cofacial bisporphyrins.

Results and Discussion

Structure and Energetics of Pacman Complexation. DPD cofacial bisporphyrins anchored by a single dibenzofuran spacer are available using the three-branch strategy originally developed by Chang[8] and elaborated by Collman.[13] Zinc insertion into the H_4(DPD) ligand proceeds in a quantitative manner using standard conditions to give the previously reported Zn_2(DPD) (**1**). The regioselective attachment of porphyrin macrocycles at the 4 and 6 positions of dibenzofuran yields a splayed DPD system that displays large vertical pocket sizes (>7.5 Å in metal−metal distances) with minimal lateral displacements of the porphyrin subunits; this architecture provides a complementary wedge-shaped host structure for pyrimidine-based guests.[43]

The complexation of 2-aminopyrimidine by **1** is readily monitored using ^{1}H NMR spectroscopy, as highlighted in Figure 1. In the presence of up to 1 equiv of the guest, two distinct sets of chemical shifts are observed between 9 and 10 ppm, corresponding to the meso protons of free host **1**

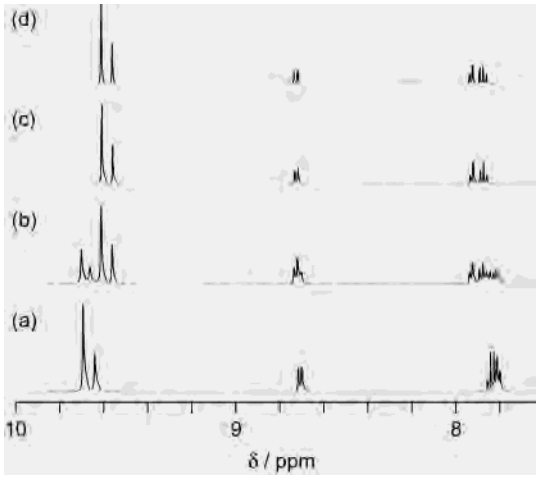

Figure 1. Selected ^{1}H NMR spectra of **1** containing (a) 0, (b) 0.67, (c) 1, and (d) 3 equiv of 2-aminopyrimidine in CD_2Cl_2 solution at 25 °C. The spectral range captures the signals for the meso protons of free host **1** and host−guest complex **2**, which are found in the range of 9−10 ppm.

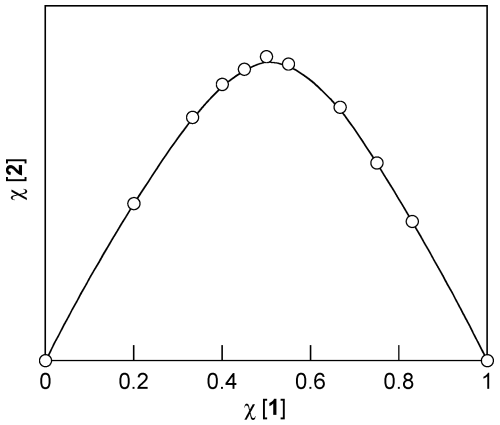

Figure 2. Job plot establishing the 1:1 stoichiometry for binding of 2-aminopyrimidine inside the cleft of host **1**. χ[**1**] and χ[**2**] are the mole fractions of host and host−guest complexes, respectively.

(δ 9.67, 9.71 ppm) and a single host−guest complex (δ 9.58, 9.63 ppm). For the latter complex, the proton signals of the guest exhibit significant upfield shifts (δ −3.70, −0.72, 2.40 ppm) compared to those of the free guest (δ 4.90, 6.62, 8.30 ppm), consistent with coordination of the bidentate pyrimidine within the cleft of dimer **1**. The formation of a single complex is observed when a 1:1 host−guest ratio is attained. Further addition of the guest produces signals only for uncomplexed pyrimidine. In addition, no changes in signal for the host−guest complex are detected in the temperature range from −20 to 40 °C. A Job plot[66] of the ^{1}H NMR titration data (Figure 2) shows that the complex is optimally formed at equimolar concentrations of porphyrin host and pyrimidine guest (i.e., a 0.5 mole fraction). Taken together, these data establish the formation of a stable 1:1 complex of **1** and 2-aminopyrimidine.

The stability of the host−guest complex allows for its isolation as an analytically pure solid on a preparative scale in good yield (85%). Material suitable for single-crystal X-ray analysis can be obtained from chloroform/methanol solutions. The structure of the host−guest complex Zn_2(DPD)(2-

(50) Nakash, M.; Clyde-Watson, Z.; Feeder, N.; Davies, J. E.; Teat, S. J.; Sanders, J. K. M. *J. Am. Chem. Soc.* **2000**, *122*, 5286−5293.
(51) Anderson, S.; Anderson, H. L.; Sanders, J. K. M. *J. Chem. Soc., Perkin Trans. 1* **1995**, 2255−2267.
(52) Anderson, S.; Anderson, H. L.; Sanders, J. K. M. *Acc. Chem. Res.* **1993**, *26*, 469−475.
(53) Anderson, H. L.; Hunter, C. A.; Meah, M. N.; Sanders, J. K. M. *J. Am. Chem. Soc.* **1990**, *112*, 5780−5789.
(54) Hunter, C. A.; Sanders, J. K. M. *J. Am. Chem. Soc.* **1990**, *112*, 5525−5534.
(55) Hunter, C. A.; Meah, M. N.; Sanders, J. K. M. *J. Am. Chem. Soc.* **1990**, *112*, 5773−5780.
(56) Hunter, C. A.; Leighton, P.; Sanders, J. K. M. *J. Chem. Soc., Perkin Trans. 1* **1989**, 547−552.
(57) Hunter, C. A.; Meah, M. N.; Sanders, J. K. M. *J. Chem. Soc., Chem. Commun.* **1988**, 694−696.
(58) Hunter, C. A.; Meah, M. N.; Sanders, J. K. M. *J. Chem. Soc., Chem. Commun.* **1988**, 692−694.
(59) Borovkov, V. V.; Lintuluoto, J. M.; Inoue, Y. *J. Am. Chem. Soc.* **2001**, *123*, 2979−2989.
(60) Brettar, J.; Gisselbrecht, J.-P.; Gross, M.; Solladié, N. *Chem. Commun.* **2001**, 733−734.
(61) Huang, X.; Borhan, B.; Rickman, B. H.; Nakanishi, K.; Berova, N. *Chem.—Eur. J.* **2000**, *6*, 216−224.
(62) Crossley, M. J.; Thordarson, P. *Angew. Chem., Int. Ed.* **2002**, *41*, 1709−1712.
(63) Uemori, Y.; Nakatsubo, A.; Imai, H.; Nakagawa, S.; Kyuno, E. *Inorg. Chem.* **1992**, *31*, 5164−5171.
(64) Richardson, D. E.; Taube, H. *J. Am. Chem. Soc.* **1983**, *105*, 40−51.
(65) Katz, H. E. *J. Org. Chem.* **1989**, *54*, 2179−2183.
(66) Connors, K. A. *Binding Constants*; Wiley: New York, 1987.

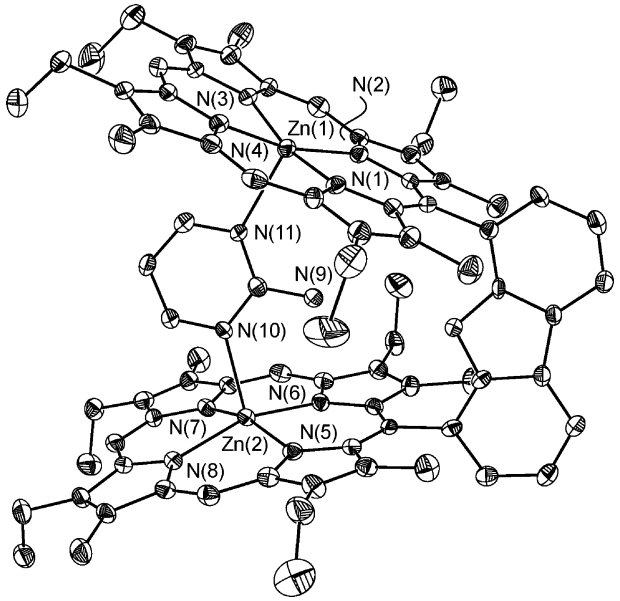

Figure 3. Crystal structure of **2**. Thermal ellipsoids are drawn at the 25% probability level. Hydrogen atoms have been omitted for clarity.

Table 1. Crystallographic Data for Zn_2(DPD)(2-aminopyrimidine) (**2**)

empirical formula	$C_{83}H_{84}Cl_9N_{11}OZn_2$
fw	1701.40
T (K)	183(2)
λ (Å)	0.710 73
cryst syst	monoclinic
space group	$P2(1)/n$
a (Å)	17.9742(3)
b (Å)	19.1934(3)
c (Å)	26.1291(10)
β (deg)	102.1760(10)
V (Å^3)	8811.4(2)
Z	4
ρ_{calcd} (g cm^{-3})	1.283
abs coeff (mm^{-1})	0.866
F(000)	3520
no. of reflns collected	25 903
independent reflns (R_{int})	8209 (0.0433)
data/restraints/params	8209/6/993
R1,[a] wR2 [b]	0.0863, 0.2434
R1,[a] wR2[b] (all data)	0.0943, 0.2503
GOF[c] on F^2	1.107

[a] $R1 = \sum||F_o| - |F_c||/\sum|F_o|$. [b] $wR2 = (\sum(w(F_o^2 - F_c^2)^2)/\sum(w(F_o^2)^2))^{1/2}$. [c] $GOF = (\sum w(F_o^2 - F_c^2)^2/(n-p))^{1/2}$ where n is the number of data refined and p is the number of parameters refined.

aminopyrimidine) (**2**) depicted in Figure 3 confirms the encapsulation of 2-aminopyrimidine inside the cavity of bisporphyrin **1**. Taken together, the molecular structures of **1** and **2** represent a rare pair of structurally homologous dizinc(II) bisporphyrin host and host−guest complexes[49,50] and consequently offer a direct structural comparison for the Pacman effect upon substrate complexation.[43]

Crystallographic data are given in Table 1, and selected geometrical measurements are given in Table 2. Trends in bond lengths and angles of macrocyclic core structures and side chains agree well with those observed in related cofacial bisporphyrins. Structural highlights of **2** in relation to **1** are as follows. The framework of free host **1** undergoes a number of conformational changes upon ligation of the pyrimidine guest to produce **2**. The binding of the guest triggers a closure of the molecule along a single longitude, affording a complex with a reduced Zn−Zn distance of 6.684 Å (Zn−Zn = 7.775 Å in free host **1**). The tightened conformation also results in compressed distances between the cofacial porphyrin meso carbons connected to the spacer (5.577 Å in **1**, 5.444 Å in **2**). For **2**, the five-coordinate Zn(II) ions adopt a square pyramidal geometry with an average Zn−$N_{pyrrole}$ bond length of 2.076 Å. Inequivalent Zn−N_{guest} bond distances are observed in the solid state (2.257 and 2.346 Å), and the corresponding zinc atoms are displaced toward the guest by 0.334 and 0.236 Å, respectively, from the corresponding N_4 macrocyclic planes. The guest is locked in a coplanar arrangement with the dibenzofuran spacer (dihedral angle = 0.4°), placing the amino nitrogen of the pyrimidine guest 3.380 Å from the oxygen atom of the dibenzofuran bridge and 3.398 Å from the nearest porphyrinic nitrogen. The key structural feature of **2** in relation to free host **1** is the small torsional twist (4.6° for **2**, 1.2° for **1**, defined as the torsion angle between the two meso-carbon to spacer bonds) between porphyrinic subunits, giving a host−guest complex in which the only notable conformational change from the free host is in the vertical direction.

The binding between **1** and 2-aminopyrimidine can also be characterized using absorption spectroscopy. The addition of 2-aminopyrimidine to dichloromethane solutions of **1** at room temperature results in noticeable red shifts for the Soret (from 399 to 406 nm) and Q-band (from 533 and 570 to 539 and 575 nm, respectively) manifolds (Figure 4), indicative of axial nitrogen coordination to a zinc(II) porphyrin.[67,68] Well-anchored isosbestic points over the entire range of binding isotherms indicate the existence of an equilibrium between the host and the 1:1 host−guest complex. Furthermore, a Hill plot[69] of $\ln[(A_I - A)/(A - A_F)]$ yields a slope of 1.00 ± 0.03, indicating a simple binding process with no cooperativity. The association constant, $K_A = 9.6(7) \times 10^7$ M^{-1}, is among the highest observed for the binding of nitrogen heterocycles to zinc(II) porphyrin based hosts[51,53−63] and is noteworthy for coordination of the relatively weak pyrimidine base ($pK_a = 3.5$).[70] The large K_A attests to (i) the efficacy of the fit induced by complementary shape-matching of the pyrimidine guest to the wedged binding site of the DPD cleft and (ii) the facile vertical Pacman closure to provide a stable host−guest adduct. The thermodynamic parameters $\Delta H° = -63(6)$ kJ mol^{-1} and $\Delta S° = -61(12)$ J mol^{-1} K^{-1} are obtained from titrations at various temperatures. Notably, the entropic penalty associated with formation of host−guest complex **2** via a single vertical Pacman motion is small in comparison to binding ditopic ligands to doubly strapped dizinc(II) porphyrin receptors ($\Delta S° \sim -100$ to 130 J mol^{-1} K^{-1}) with multiple degrees of freedom.[53−55]

Binding studies were extended to include a series of 2-substituted pyrimidines. The data collected in Table 3 show that such guests coordinate to **1** with association constants

(67) Miller, J. R.; Dorough, G. D. *J. Am. Chem. Soc.* **1952**, *74*, 3977−3981.
(68) Hambright, P. *J. Chem. Soc., Chem. Commun.* **1967**, 470−471.
(69) Hill, A. V. *J. Physiol. (London)* **1910**, *40*, pp IV−VII.
(70) Basicities (pK_a) of common heterocyclic nitrogen ligands for zinc(II) porphyrins: pyridine = 5.25, DABCO = 8.60, imidazole = 6.95, pyrazine = 0.65.

Table 2. Selected Bond Lengths (Å) and Angles (deg) Calculated for Zn_2(DPD)(2-aminopyrimidine) (**2**)

Bond Lengths (Å)							
Zn(1)−N(1)	2.064(6)	Zn(1)−N(3)	2.105(6)	Zn(2)−N(5)	2.064(6)	Zn(2)−N(7)	2.069(7)
Zn(1)−N(2)	2.067(6)	Zn(1)−N(4)	2.090(7)	Zn(2)−N(6)	2.065(6)	Zn(2)−N(8)	2.084(7)
Zn(1)−N(11)	2.262(6)	Zn(2)−N(10)	2.345(6)				
Bond Angles (deg)							
N(1)−Zn(1)−N(2)	87.4(2)	N(4)−Zn(1)−N(3)	87.0(3)	N(5)−Zn(2)−N(6)	87.8(3)	N(7)−Zn(2)−N(8)	87.6(3)
N(1)−Zn(1)−N(4)	90.0(2)	N(1)−Zn(1)−N(11)	101.7(2)	N(5)−Zn(2)−N(7)	166.7(2)	N(5)−Zn(2)−N(10)	100.9(2)
N(2)−Zn(1)−N(4)	163.0(2)	N(2)−Zn(1)−N(11)	101.8(2)	N(6)−Zn(2)−N(7)	91.0(3)	N(6)−Zn(2)−N(10)	97.0(2)
N(1)−Zn(1)−N(3)	160.3(2)	N(4)−Zn(1)−N(11)	95.2(2)	N(5)−Zn(2)−N(8)	90.7(3)	N(7)−Zn(2)−N(10)	92.4(2)
N(2)−Zn(1)−N(3)	89.8(3)	N(3)−Zn(1)−N(11)	98.0(2)	N(6)−Zn(2)−N(8)	167.3(2)	N(8)−Zn(2)−N(10)	95.7(2)

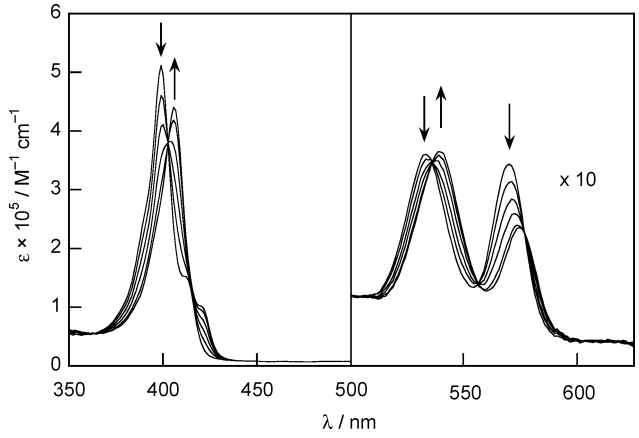

Figure 4. Absorption spectra of **1** in the presence of 0, 0.2, 0.4, 0.6, 0.8, and 1.0 equiv of 2-aminopyrimidine at 25 °C. The final spectrum does not change upon further additions of 2-aminopyrimidine.

Table 3. Association Constants for Binding of Various Pyrimidines to Zn_2(DPD) (**1**) in Dichloromethane at 25 °C

guest	K_A (M^{-1})
2-aminopyrimidine	$9.6(7) \times 10^7$
pyrimidine	$4.0(2) \times 10^4$
2-chloropyrimidine	$6.2(1) \times 10^2$
2-bromopyrimidine	$7.0(1) \times 10^2$
5-aminopyrimidine	$7.0(1) \times 10^4$

ranging over 5 orders of magnitude. The results reveal the general trend that more basic pyrimidines associate more strongly to host **1**. It is interesting to note, however, that the association constants do not directly track with the acidity of the guest; for example, significant differences in binding affinity (ca. 1400-fold) are observed for 2-aminopyrimidine and its 5-isomer despite comparable pK_a values (3.5 for the 2-isomer, 2.8 for the 5-isomer). As displayed by the structure of **2**, the 2-amino group is not within standard hydrogen-bonding distance (<3 Å) of either the dibenzofuran bridge oxygen (3.380 Å) or the porphyrin nitrogens (3.398 Å). These observed metrics suggest that subtler cavity effects may play a role in this host−guest stabilization.

To test this assertion, density functional theory (DFT) calculations were carried out to probe the origin of the stability of host−guest complex **2**. Surprisingly, Mulliken population analysis reveals the absence of significant overlap population along the internuclear axis of the 2-amino guest group and the dibenzofuran bridge oxygen, despite their proximity (3.380 Å). Instead, considerable overlap is present between the 2-aminopyrimidine nitrogen and the two proximal meso carbons C(5) and C(25) directly connected to the spacer, as well as the adjacent α-pyrrolic carbons C(4), C(6), C(24), and C(26). The sum of the Mulliken overlap populations between the amine nitrogen of 2-aminopyrimidine and the aforementioned carbon atoms is 0.108 e; for comparison, the average Zn−N_{guest} overlap population is 0.218 e. These data suggest that the origin of the thermodynamically favorable host−guest interaction is a strong noncovalent interaction between the amine nitrogen of 2-aminopyrimidine and the proximal carbons of the bisporphyrin framework, with the amine nitrogen serving as a Lewis base and the proximal porphyrin meso carbon serving as a Lewis acid. The strong noncovalent host−guest interaction is manifested in an increase in positive electronic charge of the porphyrinic subunits upon binding of the guest (−0.188 e in **1**, +0.171 e in **2**). Because binding of the pyrimidine guest to the bisporphyrin host leads to further stabilization of the host−guest complex, we view the host−guest interaction as a synergistic one.

Effects of Pacman Complexation on Excited-State Dynamics. With an understanding of the structure and energetics of Pacman complexation in hand, we set out to investigate the effects of guest binding on the excited-state dynamics of the cofacial bisporphyrin motif. For comparison with free host Zn_2(DPD) (**1**) and host−guest complex Zn_2(DPD)(2-aminopyrimidine) (**2**), we also examined the compressed Pacman system Zn_2(DPX) (**3**) and a baseline monomer Zn(OEP) (**4**) (OEP = 2,3,7,8,12,13,17,18-octaethylporphyrin), as well as a monomeric porphyrin bearing a single meso aryl ring Zn(PhEtio) (**5**) (PhEtio = 5-(4′-bromophenyl)-2,8,-13,17-tetraethyl-3,7,12,18-tetramethylporphyrin) (Chart 1).

Figure 5 depicts transient absorption spectra for **1**−**5** following a 3-ns excitation pulse at 532 nm. The zinc porphyrin compounds display similar profiles. As observed previously for their palladium analogues,[46] the key spectral features include a broad, prominent triplet excited-state absorption band and accompanying bleaching signals of the Soret and Q-bands. The energetic trends of these transient features track the corresponding ground-state electronic absorption spectra; the transient absorption maxima are collected in Table 4. The shift in the transient absorption maximum of Zn(PhEtio) from 438 to 463 nm following a 200-ns delay and the observation of biexponential decay kinetics suggest the presence of two excited-state species. As observed for the Pd analogues,[46] this result is in accordance with Albinsson's "mother−daughter" relationship[71] for two triplet excited states in which the "mother" signal arises from a porphyrin in a planar geometry and the "daughter" signal arises from a porphyrin macrocycle that exhibits a nonplanar distortion.

Chart 1

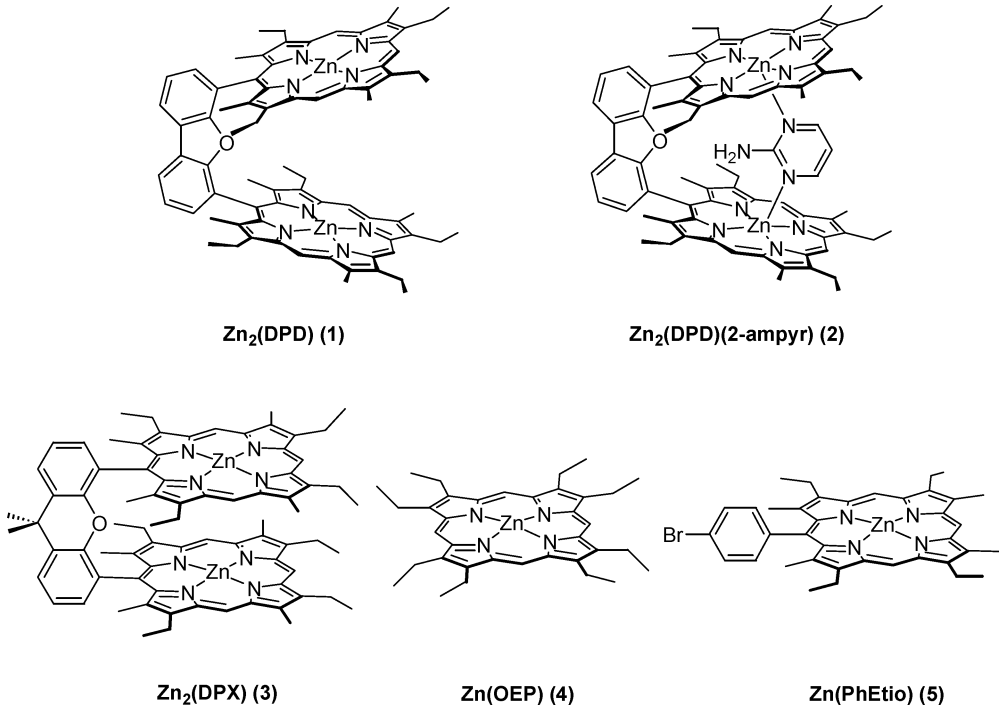

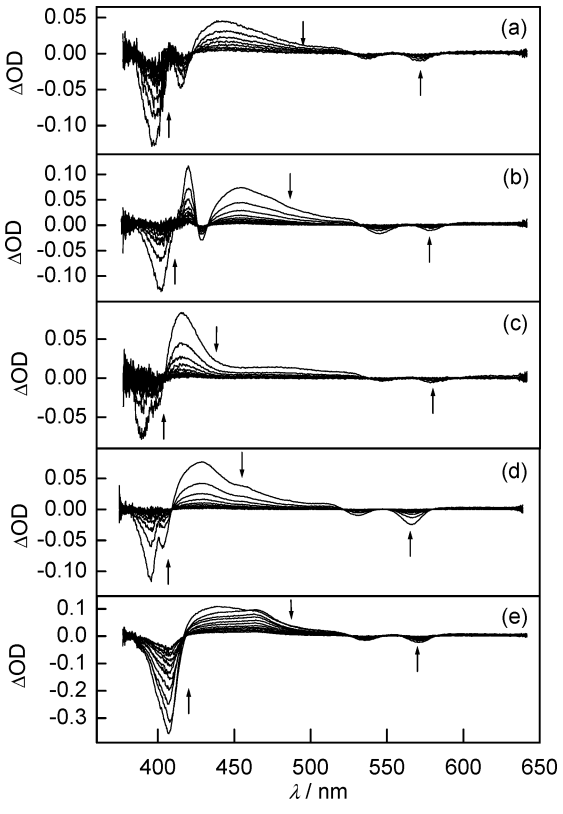

Figure 5. Transient absorption spectra of (a) Zn_2(DPD) (**1**), (b) Zn_2(DPD)-(2-aminopyrimidine) (**2**), (c) Zn_2(DPX) (**3**), (d) Zn(OEP) (**4**), and (e) Zn(PhEtio) (**5**) following excitation by a 3-ns pulse at 532 nm. Spectra in (a) are recorded at time intervals of 5 μs, spectra in (b), (c), and (d) are recorded at time intervals of 50 μs, and spectra in (e) are recorded at time intervals of 200 ns.

The transient absorption spectra of the zinc porphyrins decay on the microsecond time scale; the susceptibility of these transient species to quenching by O_2 confirms the triplet

Table 4. Transient Absorption Maxima and Decay Lifetimes of Zinc Porphyrins

	λ (nm)	τ (μs)
Zn_2(DPD) (**1**)	443	21.4(12)
Zn_2(DPD)(2-ampyr) (**2**)	451	227(8)
Zn_2(DPX) (**3**)	410	169(9)
Zn(OEP) (**4**)	427	161(5)
Zn(PhEtio) (**5**)	438, 463	1.19(1), 0.0773(15)

character of the excited states under observation. The time-resolved absorption decays are shown in Figure 6, and the measured triplet lifetimes are collected in Table 4. The general trend in the lifetimes of the zinc porphyrin monomers and dimers closely mirrors their palladium congeners.[46] The monoexponential excited-state decays of Zn_2(DPD) (**1**) and Zn_2(DPX) (**3**) occur on markedly disparate time scales, with Zn(OEP) (**4**) exhibiting a long-lived excited state resembling the DPX system; in contrast, the shortened triplet lifetimes observed for the DPD compound and Zn(PhEtio) (**5**) are a consequence of torsional motions about their $C_{meso}-C_{aryl\ bridge}$ bonds that lead to nonplanar distortions of the porphyrin macrocycle, which in turn enhances nonradiative decay pathways. We believe that this motion is suppressed in the DPX case; a compressed porphyrin−porphyrin distance for the DPX scaffold likely hinders rotation of macrocyclic subunits with respect to the aryl bridge owing to the steric encumbrance arising from the other proximate porphyrin. The most striking result from these photophysical studies is the substantial increase in the triplet excited-state lifetime for the host−guest complex Zn_2(DPD)(2-aminopyrimidine) (**2**) over free host **1**. This finding confirms that substrate prebinding inside the cofacial cavity serves to suppress the torsional librations that

(71) Andreasson, J.; Zetterqvist, H.; Kajanus, J.; Martensson, J.; Albinsson, B. *J. Phys. Chem. A* **2000**, *104*, 9307−9314.

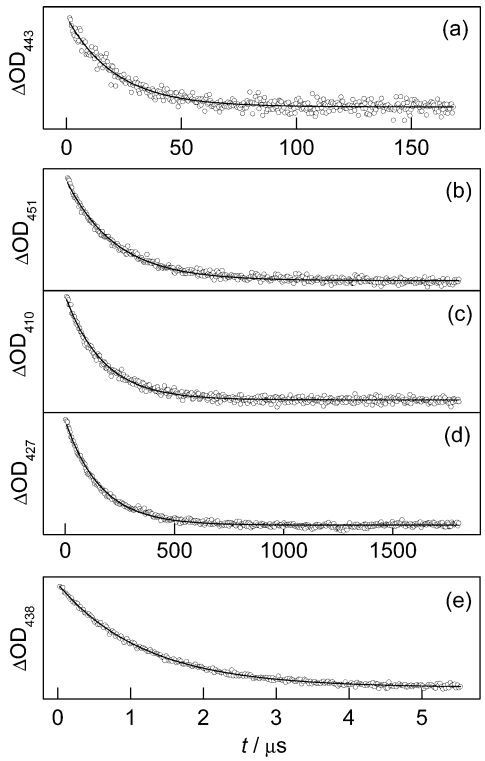

Figure 6. Transient absorption decays monitored at ΔOD maximum of (a) Zn_2(DPD) (**1**), (b) Zn_2(DPD)(2-aminopyrimidine) (**2**), (c) Zn_2(DPX) (**3**), (d) Zn(OEP) (**4**), and (e) Zn(PhEtio) (**5**) following excitation by a 3-ns pulse at 532 nm.

promote quenching of the triplet excited state of Pacman motifs.

Concluding Remarks

The Pacman effect allows the cofacial bisporphyrin motif to create a suitable microenvironment for mediating dynamic host−guest chemistry for catalysis. In particular, the DPD architecture has exceptional vertical flexibility for a pillared cofacial system while preserving a face-to-face arrangement of macrocyclic subunits, a feature that is central to its ability to mediate both multielectron reduction and oxidation chemistry. However, this structural attribute presents a significant challenge for translating the reactivity of the DPD platform to efficient excited-state catalysis; namely, the large torsional flexibility associated with its splayed structural motif has a detrimental effect on its excited-state lifetime. To address this issue, we have utilized the Pacman effect to afford a novel approach for tuning the excited-state dynamics of the cofacial bisporphyrin motif. Specifically, we have elaborated the host−guest chemistry of Pacman platforms using zinc(II) derivatives and basic nitrogen donors. Binding studies clearly demonstrate that the vertical Pacman flexibility of DPD is accompanied by a small conformational energy, thus affording an effective pocket for substrate binding. When the bisporphyrin host is confined to a single vertical degree of freedom, the entropic gain of DPD over traditional bisporphyrin templates is observed to be roughly 60 J mol^{-1} K^{-1} with negligible differences in enthalpy, leading to unprecedented binding affinities for the weakly basic pyrimidine substrate. Pacman complexation provides an effective supramolecular strategy for enhancing the excited-state properties of the cofacial bisporphyrin motif. When the motions of porphyrin rotation upon photon absorption are controlled, the excited-state lifetime of the DPD scaffold is extended by an order of magnitude over the unbound Pacman construct. These results provide further evidence that the broad reactivity of the DPD platform is due to its ability to undergo a substantial Pacman rearrangement along a single longitudinal coordinate upon ligation while maintaining a cofacial presentation of porphyrin subunits to afford bimetallic reactivity and demonstrate that dynamic host−guest chemistry can be applied toward tuning excited-state properties. Efforts to exploit the Pacman effect for thermal and photochemical multielectron catalysis are in progress.

Experimental Section

Materials. Solvents used for synthesis were of reagent grade or better and were dried according to standard methods.[72] Spectroscopic experiments employed toluene or dichloromethane (spectroscopic grade, Burdick & Jackson), which were stored over 4 Å molecular sieves. Zn_2(DPD) (**1**) and Zn_2(DPX) (**3**) were available from previous studies.[39,43] All other reagents were used as received.

Zn_2(DPD)(2-aminopyrimidine) (2). Chloroform (10 mL) was added to a solid mixture of Zn_2(DPD) (**1**) (50 mg, 0.04 mmol) and 2-aminopyrimidine (3.8 mg, 0.04 mmol). The resulting solution was layered with hexanes (20 mL) and placed in a freezer at −20 °C for 2 days. A crop of ruby-red crystals was isolated by gravity filtration, washed with cold hexanes (2 × 10 mL), and dried under vacuum to furnish analytically pure **2** (46 mg, 85% yield). ^{1}H NMR (500 MHz, CD_2Cl_2, 25 °C): δ 9.63 (s, 4H, meso), 9.58 (s, 2H, meso), 8.74 (d, 2H, ArH), 7.94 (t, 2H, ArH), 7.88 (d, 2H, ArH), 3.72−3.87 (m, 16H, CH_2), 3.30 (s, 12H, CH_3), 2.43 (br s, 1H, PymH), 2.32 (s, 12H, CH_3), 1.58 (t, 12H, CH_3), 1.51 (t, 12H, CH_3), −0.73 (m, 2H, PymH), −3.70 (br s, 2H, NH_2). Anal. Calcd for $C_{80}H_{81}N_{11}OZn_2$: C, 71.53; H, 6.08; N, 11.47. Found: C, 71.16; H, 6.03; N, 11.53.

General Details of X-ray Data Collection and Reduction. X-ray diffraction data were collected using a Siemens Circle 3 diffractometer equipped with a charge-coupled device (CCD) detector. Measurements were carried out at −90 °C using Mo Kα (λ = 0.710 73 Å) radiation, which was wavelength selected with a single-crystal graphite monochromator. Four sets of data were collected using ω scans and a −0.3° scan width. All calculations were performed using a PC workstation. The data frames were integrated to *hkl*/intensity, and final unit cells were calculated using the SAINT v.4.050 program from Siemens. The structures were solved and refined with the SHELXTL v.5.03 suite of programs developed by G. M. Sheldrick and Siemens Industrial Automation, Inc., 1995. Plots were drawn using XP.

X-ray Structure of 2. A 0.28 mm × 0.42 mm × 0.50 mm ruby-red crystal was obtained by slow diffusion of hexane into a chloroform solution of the complex. The crystal was coated in Paratone N and mounted onto a glass fiber. The structure was solved by direct methods in conjunction with standard difference Fourier techniques. Hydrogen atoms were placed in calculated positions using a standard riding model and were refined isotropically. Three chloroform molecules were found in the crystal, and one of them was found to be disordered. This molecule was assigned half

(72) Armarego, W. L. F.; Perrin, D. D. *Purification of Laboratory Chemicals*, 4th ed.; Butterworth-Heinmann: Oxford, 1996.

occupancy at two symmetry-equivalent positions. Restraints were applied to one solvent molecule by using the SADI command of SHELXTL. The largest peak and hole in the difference map were 1.384 and −0.708 e Å^{-3}, respectively.

Physical Measurements. ^{1}H NMR spectra were collected in $CDCl_3$, CD_2Cl_2, or d_8-toluene (Cambridge Isotope Laboratories) at the MIT Department of Chemistry Instrumentation Facility (DCIF) using either a Mercury 300 or an Inova 500 spectrometer. All chemical shifts are reported using the standard δ notation in parts-per-million; positive chemical shifts are shifts to higher frequency from the given reference. Mass spectral analyses were carried out at the MIT Department of Chemistry Instrumentation Facility and the University of Illinois Mass Spectrometry Laboratory. Elemental analyses were performed at the University of Illinois Microanalytical Laboratory.

Absorption spectra were obtained using a Cary-17 spectrophotometer modified by On-Line Instrument Systems (OLIS) to include computer control, a Spectral Instruments 440 spectrophotometer, or a Hewlett-Packard 8453 spectrophotometer equipped with a Hewlett-Packard 89090A Peltier temperature control accessory. UV−visible titrations were carried out by the addition of small amounts of guest aliquots (1 μL) into dilute solutions (ca. 10^{-6} M, 2−3 mL) of porphyrin. Titrations were carried out in at least triplicate. Association constants (K_A) were obtained from plots of [G] against [G]/ΔA where [G] = concentration of guest and ΔA is the difference in absorbance of the porphyrin host in the absence and presence of guest and were determined independently from data at three different wavelengths. Enthalpies and entropies for ligation were determined by standard van't Hoff plots of ln K_A vs $1/T$ for six temperatures ranging from 283 to 333 K.

Samples for time-resolved spectroscopic measurements were contained within an optical cell equipped with a solvent reservoir and a Starna Cells, Inc. 1-cm path length clear fused-quartz cell. The two chambers are isolated from each other by a high-vacuum Teflon valve and from the environment with a second high-vacuum Teflon valve. Samples were dissolved in dichloromethane (10 μM), and the solution was degassed by four freeze−pump−thaw cycles (1×10^{-5} Torr). Transient absorption spectra and excited-state lifetimes of all porphyrins were measured on a nanosecond laser system described previously.[46] The excitation power impinging on the sample was 8 mW.

Computational Methods. Density functional theory (DFT) calculations were carried out using the Amsterdam density functional program.[73−75] Gradient corrections were introduced using the Becke exchange functional (B)[76] and the Lee−Yang−Parr (LYP) correlation functional.[77] Relativistic corrections were included using the scalar zero-order regular approximation (ZORA).[78−80] Carbon, hydrogen, and oxygen were described by a Slater type orbital double-ζ basis set augmented with one polarization function. Nitrogen and zinc were described by a triple-ζ basis set augmented by two and one polarization functions, respectively. Non-hydrogen atoms were assigned a relativistic frozen core potential, treating as core the shells up to and including 2p for Zn and 1s for C, N, and O. Electronic charges were computed by integrating the orthogonalized-fragment density over the Voronoi cell.

Acknowledgment. C.J.C. gratefully acknowledges the National Science Foundation and the MIT/Merck Foundation for predoctoral fellowships. Z.-H.L. thanks the MIT Undergraduate Research Opportunities Program (UROP) for support and the National Science and Technology Board (Singapore) for an undergraduate scholarship. The National Institutes of Health (Grant GM 47274) and the National Science Foundation (Grant CHE-0132680) provided funding for this work.

Supporting Information Available: X-ray crystallographic files in CIF format. This material is available free of charge via the Internet at http://pubs.acs.org.

IC034750W

(73) *ADF2000.02*; Vrije Universiteit Amsterdam: Amsterdam, The Netherlands, 1999.
(74) Baerends, E. J.; Ellis, D. E.; Ros, P. *Chem. Phys.* **1973**, *2*, 41−51.
(75) Te Velde, G.; Bickelhaupt, F. M.; Baerends, E. J.; Fonseca Guerra, C.; Van Gisbergen, S. J. A.; Snijders, J. G.; Ziegler, T. *J. Comput. Chem.* **2001**, *22*, 931−967.
(76) Becke, A. D. *Phys. Rev. A* **1988**, *38*, 3098−3100.
(77) Lee, C.; Yang, W.; Parr, R. G. *Phys. Rev. B* **1988**, *37*, 785−789.
(78) van Lenthe, E.; Baerends, E. J.; Snijders, J. G. *J. Chem. Phys.* **1993**, *99*, 4597−4610.
(79) van Lenthe, E.; van Leeuwen, R.; Baerends, E. J.; Snijders, J. G. *Int. J. Quantum Chem.* **1996**, *57*, 281−293.
(80) van Lenthe, E.; Ehlers, A.; Baerends, E. J. *J. Chem. Phys.* **1999**, *110*, 8943−8953.